Available online at www.sciencedirect.com
SCIENCE DIRECT®
Journal of Magnetic Resonance 171 (2004) 324–329
JMR Journal of Magnetic Resonance
www.elsevier.com/locate/jmr

Analysis of the magic asymmetric gradient stimulated echo sequence with shaped gradients

Phillip Zhe Sun[a,b,*], Seth A. Smith[a,c], Jinyuan Zhou[a,b]

[a] F. M. Kirby Research Center for Functional Brain Imaging, Kennedy Krieger Institute, Baltimore, MD 21205, United States
[b] Department of Radiology, Johns Hopkins University School of Medicine, Baltimore, MD 21205, United States
[c] Department of Biophysics and Biophysical Chemistry, Johns Hopkins University School of Medicine, Baltimore, MD 21205, United States

Received 16 March 2004; revised 8 September 2004
Available online 12 October 2004

Abstract

Recently a 13-interval magic asymmetrical gradient stimulated echo (MAGSTE) sequence has been proposed for accurate displacement measurements in the presence of spatially varying background gradients. In this paper, the commonly used trapezoidal and sine shaped gradients are studied for the MAGSTE sequence, and the magic asymmetrical gradient ratio and *b*-factor are provided. The derivation enables the MAGSTE sequence to be implemented on systems with non-negligible gradient rise times.

Keywords: PGSTE; MAGSTE; Diffusion; Heterogeneous media; Heterogeneous structure; Background gradient

1. Introduction

Pulsed field gradient (PFG) NMR has been an important method for measuring molecular displacement [1,2]. For molecular diffusion processes in homogeneous samples of infinite size, the spin density is constant and its displacement propagator is Gaussian. Under these conditions the diffusion attenuation can be written as:

$$\frac{E(g_a)}{E(0)} = \exp\{-D(\gamma \cdot g_a \cdot \delta)^2 \cdot (\Delta - \delta/3)\}, \quad (1)$$

where $E(0)$ and $E(g_a)$ are the echo intensities with the applied rectangular gradient at the strength of 0 and g_a, respectively; D is the diffusion coefficient; δ is the gradient pulse duration; and Δ is the diffusion time between the leading edges of the pulsed gradients. Eq. (1) is accurate if the spins experience only the applied external gradients. However, in addition to the applied gradients, there are also background gradients (g_b) created by the microscopic and/or macroscopic heterogeneity of inhomogeneous samples. Stejskal and Tanner [1] studied the combined effects of a time-dependent magnetic field gradient and a constant gradient on the measurement of the molecular diffusion using a spin echo experiment and found the echo intensity attenuation to be

$$\frac{E(g_a)}{E(0)} = \exp\left\{-\gamma^2 D\left\{\frac{2}{3}\tau^3 g_b^2 + \delta^2\left(\Delta - \frac{1}{3}\delta\right)g_a^2 - \delta\left[(t_1^2 + t_2^2) + \delta(t_1 + t_2) + \frac{2}{3}\delta^2 - 2\tau^2\right] g_a \cdot g_b\right\}\right\}, \quad (2)$$

where τ is half the duration of the echo time, t_1 is the pre-gradient delay, and $t_2 = 2\tau - (t_1 + \Delta + \delta)$ is the time between the end of the second gradient pulse and the peak of the echo. According to Eq. (2), it is necessary to know the background gradient to measure the diffusion constant precisely. Assuming that the background gradients are spatially constant along the route of the spins' displacement and can be modeled by a zero-mean

* Corresponding author.
E-mail address: pzhesun@mri.jhu.edu (P.Z. Sun).

1090-7807/$ - see front matter
doi:10.1016/j.jmr.2004.09.005

Gaussian function with its variance σ across the sample, Zhong and Gore [3] showed that the diffusion measurement from the spin echo experiment can be written as

$$D_{\text{app}} = D\left[1 - \frac{1}{2}D(\gamma\sigma)^2(TE - \Delta/2)^2\Delta\right], \quad (3)$$

which is a function of the background gradient, echo time and evolution time. They also showed that the echo intensity had a non-linear dependence on the diffusion time in phantoms and various types of excised tissues, demonstrating that background gradients can affect the diffusion measurements.

To improve the measurement, Karlicek and Lowe [4] developed an alternating pulse filed gradient (APFG) sequence, which strongly reduced the effect of the background gradients. Cotts et al. [5] proposed a number of sequences based on bipolar gradients and stimulated echo (STE) to deal with the case of short transverse relaxation times. Latour et al. [6] designed a more effective sequence combining the APFG and STE sequence. All these sequences can suppress the artifacts from constant background gradients and have been reviewed by Johnson [2]. However, the theoretical analysis and experimental evidence provided by Seland et al. [7] showed that the application of the bipolar PGSTE may fail to suppress all of the cross terms between the background and the applied gradients for long evolution times. Recently, Sun et al. [8,9] reported an asymmetric diffusion coding scheme that suppresses the cross terms between the applied and the background gradients during the encoding and decoding interval independently. This allows an accurate diffusion measurement even when spins displace to positions where the local background gradients are uncorrelated after the storage interval. This coding scheme has been demonstrated in phantoms with simulated background gradients [8,9] and naturally generated background gradients [10]. In this paper, the magic asymmetric gradient ratio (MAGR) and the b-factor for commonly used trapezoidal and sine shaped gradients are derived and analyzed such that the magic asymmetric gradient stimulated echo (MAGSTE) sequence can be implemented on systems with non-negligible gradient rise time.

2. MAGSTE sequence analysis

2.1. General

Due to the symmetry of the MAGSTE sequence (Fig. 1) in k-space, MAGR can be derived by analyzing the diffusion processes during either the encoding or decoding interval [11]. In this study, we choose the encoding interval for the analysis. The wave-number k and b-factor are defined, respectively, as:

$$k(t) = k(0) + \gamma \cdot \int_0^t \{g_{\text{a}}(t') + g_{\text{b}}(t')\}\,\mathrm{d}t',$$
$$b(t) = b(0) + \int_0^t \left\{k(0) + \gamma\int_0^{t'}(g_{\text{a}}(t'') + g_{\text{b}}(t''))\,\mathrm{d}t''\right\}^2 \mathrm{d}t', \quad (4)$$

where $k(0)$ and $b(0)$ are the wave-number and b-factor at the beginning of the diffusion interval under consideration. For background gradients whose correlation time is longer than the coding interval 2τ, they can be modeled by a constant gradient g_{b}. To derive the MAGR, the b-factor needs to be computed throughout the encoding interval. In general, the b-factor includes the cross term of the external gradient and background gradients and their respective quadratic terms

$$b(2\tau) = f(g_a^2, g_a g_{\text{b}}, g_{\text{b}}^2, \eta, \ldots), \quad (5)$$

where η is the MAGR, defined as the ratio of the two pulsed gradients during the coding interval, namely, $\eta = g_{\text{a1}}/g_{\text{a2}}$ or $g_{\text{a4}}/g_{\text{a3}}$ (Fig. 1). The MAGR can then be treated as a free parameter to null the cross term at the end of the coding interval. The quadratic background gradient term will drop out, when the echo intensity is normalized to that acquired without the external gradients. For conventional PGSTE sequences, the cross term during the encoding time needs to be compensated for during the decoding time, which requires that spins experience the same background gradient throughout the echo time. Thus, the nulling of the cross term right before the storage time allows the constraint to be relaxed to the coding interval only. Because the storage time can be as long as the longitudinal relaxation time, the MAGSTE sequence provides an approach to measure the displacement propagator accurately even when the storage time is longer than the correlation time of the background gradients.

2.2. Trapezoidal shaped gradients

Because of the finite rise time of the external gradient, even with good pre-emphasis compensation, shaped gradients are widely regarded as having higher wave form fidelity and less eddy currents than rectangular gradients. In addition, trapezoidal gradients can have very high spatial encoding efficiencies and are easy to implement. Here, we choose them for the MAGSTE sequence analysis. The temporal symmetry in k-space around the center of the storage time guarantees the same MAGR for both the encoding and decoding intervals even when the equality of pre- and post-gradient delays δ_1 and δ_2 is not maintained. Thus, the notation of δ_1 and δ_2 is chosen to be consistent with those used by Sun et al. [8,9]. The mathematical description of the applied gradients between the excitation and the first refocusing pulse is given as below

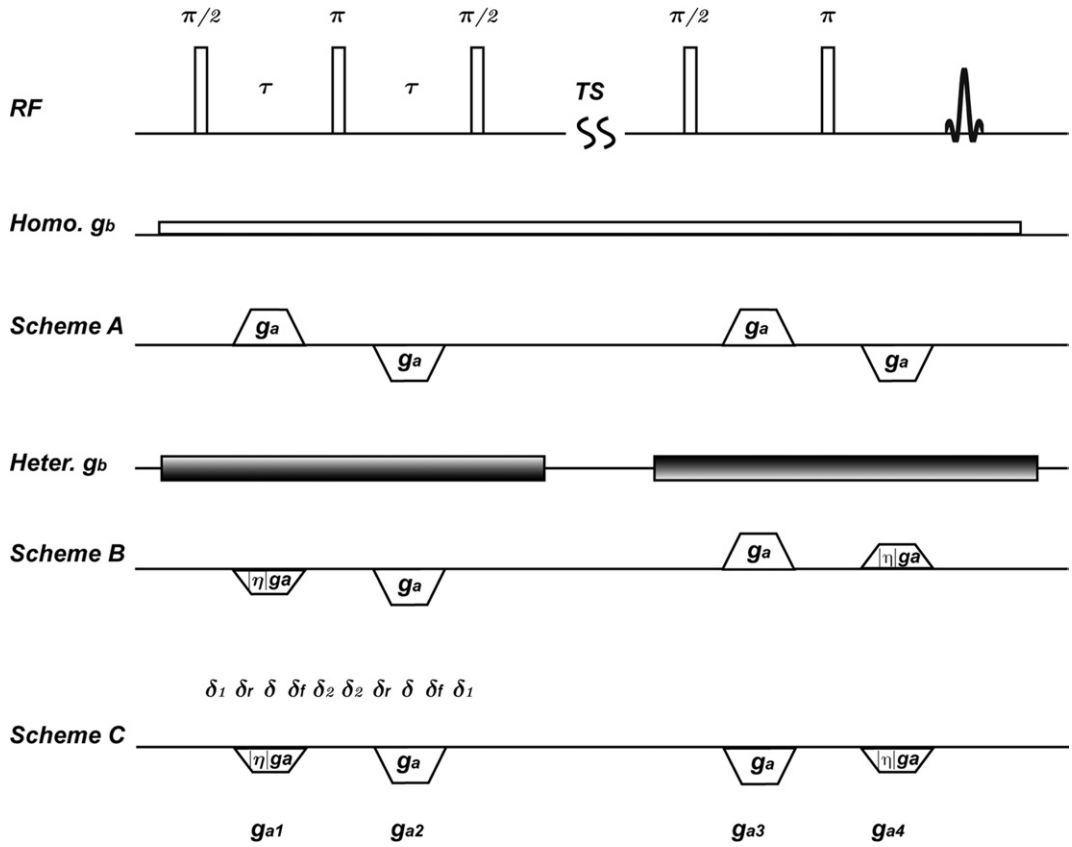

Fig. 1. The conventional 13-interval PGSTE sequence with bipolar gradients of equal amplitude (Scheme A) and MAGSTE sequence (Schemes B and C) whose two lateral pulsed gradients are modulated by the MAGR. If the background gradient is described by a constant gradient g_b, all coding schemes can correct its effect upon the diffusion measurement. When the variation of the background gradient is modeled by a correlation function, Scheme A fails to suppress all the background gradient effects. Because the cross term of background and applied gradient is compensated for during the encoding and decoding interval independently, the MAGSTE sequence can measure the diffusion accurately even with a change of the decoding gradient polarity.

$$
\begin{aligned}
&g = 0 \quad \text{for} \quad 0 < t < \delta_1 \\
&g = \eta \cdot g_a \cdot \frac{t-\delta_1}{\delta_r} \ \text{for} \ \delta_1 < t < \delta_1 + \delta_r \\
&g = \eta \cdot g_a \ \text{for} \ \delta_1 + \delta_r < t < \delta_1 + \delta_r + \delta \\
&g = \eta \cdot g_a \cdot \left(1 - \frac{t-(\delta_1+\delta_r+\delta)}{\delta_f}\right) \\
&\quad \text{for} \quad \delta_1 + \delta_r + \delta < t < \delta_1 + \delta_r + \delta + \delta_f \\
&g = 0 \quad \text{for} \quad \delta_1 + \delta_r + \delta + \delta_f < t < \tau,
\end{aligned}
\tag{6}
$$

where δ_r and δ_f are the rise and fall time of the trapezoidal gradient, respectively. The applied gradients during the second half of the encoding interval are given by

$$
\begin{aligned}
&g = 0 \ \text{ for } \ \tau < t < \tau + \delta_1 \\
&g = -g_a \cdot \frac{t-(\tau+\delta_1)}{\delta_r} \ \text{ for } \ \tau + \delta_1 < t < \tau + \delta_1 + \delta_r \\
&g = -g_a \ \text{ for } \ \tau + \delta_1 + \delta_r + < t < \tau + \delta_1 + \delta_r + \delta \\
&g = -g_a \cdot \left(1 - \frac{t-(\tau+\delta_1+\delta_r+\delta)}{\delta_f}\right) \\
&\quad \text{for } \ \tau + \delta_1 + \delta_r + \delta < t < \tau + \delta_1 + \delta_r + \delta + \delta_f \\
&g = 0 \ \text{ for } \ \tau + \delta_1 + \delta_r + \delta + \delta_f < t < 2 \cdot \tau.
\end{aligned}
\tag{7}
$$

Furthermore, the background gradient during the coding interval is modeled by a constant gradient:

$$
g = g_b \quad \text{for} \quad 0 < t < 2 \cdot \tau. \tag{8}
$$

Evolutions of the wave-number and b-factor are derived by substituting Eqs. (6)–(8) into Eqs. (4) and (5), and the results are listed in Tables 1 and 2, respectively. Because the b-factor is very lengthy, only its incremental value for each segmented interval is given. In all derivations, we assume that the gradient rise time is equal to the fall time. At the end of the encoding interval, the b-factor can be shown to be

$$
b(2\tau) = -\gamma^2 (A \cdot g_a^2 + B \cdot g_b^2 + C \cdot g_a \cdot g_b), \tag{9}
$$

where A, B, and C are functions of the MAGR and time intervals:

$$
\begin{aligned}
A = 1/60\{&20\delta^3(1+\eta(3+4\eta)) + 30\delta^2(4\eta^2\delta_2 + 2(1+\eta)^2\delta_1 \\
&+ (3+\eta(8+11\eta))\delta_r) + 5\delta\delta_r(48\eta^2\delta_2 + 24(1+\eta)^2\delta_1 \\
&+ (23+\eta(60+83\eta))\delta_r) + 2\delta_r^2(60\eta^2\delta_2 + 30(1+\eta)^2\delta_1 \\
&+ (23+\eta(60+83\eta))\delta_r)\},
\end{aligned}
\tag{10}
$$

Table 1
The evolution of the wave-number k during the encoding interval of the MAGSTE sequence

Segment interval	Wave-number k
$t=\delta_1$	$\gamma g_b\cdot\delta_1$
$t=\delta_1+\delta_r$	$\gamma g_b\cdot(\delta_1+\delta_r)+\eta\gamma g_a\delta_r/2$
$t=\delta_1+\delta_r+\delta$	$\gamma g_b\cdot(\delta_1+\delta_r+\delta)+\eta\gamma g_a(\delta_r+2\delta)/2$
$t=\delta_1+\delta_r+\delta+\delta_f$	$\gamma g_b\cdot(\delta_1+2\delta_r+\delta)+\eta\gamma g_a(\delta_r+\delta)$
$t=\tau$	$\gamma g_b\cdot\tau+\eta\gamma g_a(\delta_r+\delta)$
$t=\tau+\delta_2$	$-\gamma g_b\cdot(\delta_1+2\delta_r+\delta)-\eta\gamma g_a(\delta_r+\delta)$
$t=\tau+\delta_2+\delta_r$	$-\gamma g_b\cdot(\delta_1+\delta_r+\delta)-\gamma g_a\cdot(\delta_r/2+\eta(\delta+\delta_r))$
$t=\tau+\delta_2+\delta_r+\delta$	$-\gamma g_b\cdot(\delta_1+\delta_r)-\gamma g_a\cdot(\delta/2+(\eta+1/2)(\delta+\delta_r))$
$t=\tau+\delta_2+\delta_r+\delta+\delta_f$	$-\gamma g_b\delta_1-\gamma g_a\cdot(\eta+1)(\delta+\delta_r)$
$t=2\tau$	$-\gamma g_a\cdot(\eta+1)(\delta+\delta_r)$

After the refocusing pulse, the wave-number polarity is flipped. The wave-number due to the background gradient is refocused during the second half of the encoding interval. Thus, the wave-number does not depend on the background gradient at the end of the encoding period.

$$B=2/3(\delta+\delta_1+\delta_2+2\delta_r)^3, \tag{11}$$

$$\begin{aligned}C=1/6(\delta+\delta_r)\{&12\eta\delta_2^2+6(1+\eta)\delta_1^2+2(1+5\eta)\delta^2\\&+12\delta_1(\delta_r+2\eta\delta_2+3\eta\delta_r)+\delta_r(7\delta_r+48\eta\delta_2+41\eta\delta_r)\\&+\delta(7\delta_r+24\eta\delta_2+41\eta\delta_r+6(1+3\eta)\delta_1)\}.\end{aligned} \tag{12}$$

To suppress the cross term in Eq. (9) such that the coupling is removed at the end of the encoding interval, the coefficient C of the cross term is set to be zero. The solution for the MAGR is

$$\eta=-\frac{2\delta^2+6\delta_1(\delta+\delta_1)+\delta_r(12\delta_1+7(\delta_r+\delta))}{\delta(10\delta+18\delta_1+24\delta_2+41\delta_r)+6\delta_1(\delta_1+4\delta_2+6\delta_r)+12\delta_2(\delta_2+4\delta_r)+41\delta_r^2}. \tag{13}$$

Because the quadratic term of the background gradients is absent, and the cross term is zero after setting the MAGR according to Eq. (13), the b-factor at the echo time depends on the applied gradient only:

$$\begin{aligned}b(\mathrm{TS}+4\tau)=\frac{\gamma^2g_a^2}{30}\{&20\delta^3(1+(3+4\eta)\eta)+30\delta^2(3\delta_r\\&+(1+\eta)^2(\mathrm{TS}+2\delta_1)+\eta(4\eta\delta_2+(8\\&+11\eta)\delta_r))+5\delta\delta_r(23\delta_r+12(1+\eta)^2\\&\times(\mathrm{TS}+2\delta_1)+\eta(48\eta\delta_2+(60+83\eta)\delta_r))\\&+2\delta_r^2(23\delta_r+15(1+\eta)^2(\mathrm{TS}+2\delta_1)\\&+\eta(60\eta\delta_2+(60+83\eta)\delta_r))\},\end{aligned} \tag{14}$$

where TS is the storage time between the second and third excitation pulse (Fig. 1).

2.3. Sine shaped gradients

We provide the results for sine shaped gradients without the stepwise derivation. The MAGR is

$$\eta=-\frac{(\pi^2-4)\delta^2+2\pi^2\delta\delta_1+2\pi^2\delta_1^2}{(4+3\pi^2)\delta^2+2\pi^2\delta(3\delta_1+4\delta_2)+2\pi^2(\delta_1^2+4\delta_1\delta_2+2\delta_2^2)}, \tag{15}$$

where δ is the duration of the sine gradient. The b-factor at the echo time is given as

$$\begin{aligned}b(\mathrm{TS}+4\tau)=\frac{\gamma^2g_a^2\delta^2}{\pi^2}\{&3\delta+4\cdot\mathrm{TS}+8(\delta_1+\eta\\&\times(\delta+2\delta_1+\mathrm{TS}))+\eta^2(11\delta+4\\&\cdot(4\delta_2+2\delta_1+\mathrm{TS}))\},\end{aligned} \tag{16}$$

where g_a is the amplitude of the sine shaped gradient.

Table 2
The evolution of the b-factor during the encoding interval of the MAGSTE sequence

Segment interval	Incremental b-factor
$0<t<\delta_1$	$\frac{1}{3}\gamma^2g_b^2\delta_1^3$
$\delta_1<t<\delta_1+\delta_r$	$\frac{\gamma^2}{60}\delta_r\{20g_b^2(3\delta_1^2+3\delta_1\delta_r+\delta_r^2)+5\eta g_ag_b\delta_r(4\delta_1+3\delta_r)+3(\eta g_a\delta_r)^2\}$
$\delta_1+\delta_r<t<\delta_1+\delta_r+\delta$	$\frac{\gamma^2}{24(g_b+\eta g_a)}\{-(2g_b(\delta_1+\delta_r)+\eta g_a\delta_r)^3+(2g_b(\delta_1+\delta_r+\delta)+\eta g_a(\delta_r+2\delta))^3\}$
$\delta_1+\delta_r+\delta<t<\delta_1+\delta_r+\delta+\delta_f$	$\frac{\gamma^2}{60}\delta_r\{20g_b^2(3(\delta_1+\delta)^2+9(\delta_1+\delta)\delta_r+7\delta_r^2)+5\eta g_ag_b(24\delta(\delta+\delta_1)$ $+4\delta_r(14\delta+5\delta_1)+31\delta_r^2)+(\eta g_a)^2(60\delta^2+100\delta\delta_r+43\delta_r^2)\}$
$\delta_1+\delta_r+\delta+\delta_f<t<\tau$	$\frac{\gamma^2}{3g_b}\{-(g_b(\delta+\delta_1+2\delta_r)+\eta g_a(\delta+\delta_r))^3+(g_b(\delta+\delta_1+\delta_2+2\delta_r)$ $+\eta g_a(\delta+\delta_r))^3\}$
$\tau<t<\tau+\delta_2$	$\frac{\gamma^2}{3g_b}\{-(g_b(\delta+\delta_1+2\delta_r)+\eta g_a(\delta+\delta_r))^3+(g_b(\delta+\delta_1+\delta_2+2\delta_r)$ $+\eta g_a(\delta+\delta_r))^3\}$
$\tau+\delta_2<t<\tau+\delta_2+\delta_r$	$\frac{\gamma^2}{60}\delta_r\{3g_a^2\delta_r^2-15g_ag_b\delta_r^2-60g_b\delta_r(g_b(\delta+\delta_1+2\delta_r)+\eta g_a(\delta+\delta_r))$ $+60(g_b(\delta+\delta_1+2\delta_r)+\eta g_a(\delta+\delta_r))^2+20\delta_r(g_b^2\delta_r+g_ag_b(\delta+\delta_1+2\delta_r)+\eta g_a^2(\delta+\delta_r))\}$
$\tau+\delta_2+\delta_r<t<\tau+\delta_2+\delta_r+\delta$	$\frac{\gamma^2}{24(-g_a+g_b)}\{(2g_b(\delta_1+\delta_r+\delta)+g_a(\delta_r+2\eta(\delta_r+\delta)))^3-(2g_b(\delta_1+\delta_r)+g_a(2\delta+\delta_r+2\eta(\delta_r+\delta)))^3\}$
$\tau+\delta_2+\delta_r+\delta<t<\tau+\delta_2+\delta_r+\delta+\delta_f$	$\frac{\gamma^2\delta_r}{60}\{20g_b^2(3\delta_1^2+3\delta_1\delta_r+\delta_r^2)+5g_ag_b(12\delta(\delta_r+2\delta_1)(1+\eta)$ $+\delta_r(20\delta_1+9\delta_r+12\eta(2\delta_1+\delta_r)))+g_a^2(60\delta^2(1+\eta)^2+20\delta\delta_r(1+\eta)(5+6\eta)+\delta_r^2(43+20\eta(5+3\eta)))\}$
$\tau+\delta_2+\delta_r+\delta+\delta<t<2\tau$	$\frac{\gamma^2}{3g_b}\{-(g_a(1+\eta)(\delta+\delta_r))^3+(g_b\delta_1+g_a(\delta+\delta_r)(1+\eta))^3\}$

2.4. Compatibility with previous results

To examine the results, we show that the above derivation is equivalent to the familiar Stejskal–Tanner equation, and consistent with the results derived by Sun et al. [8,9] and Galvosas et al. [10]:

(i) For the bipolar PGSTE sequence (13-interval PGSTE) [5], its equivalent MAGR is equal to unity. In th e absence of the background gradients, if the rise time of the trapezoidal gradient, pre-gradient delay and post-gradient delay are zero, Eq. (14) can be simplified to

$$b(\mathrm{TS}+4\tau)=(2\gamma g_a\delta)^2\left(\mathrm{TS}+2\delta-\frac{2\delta}{3}\right). \tag{17}$$

(ii) For the 9-interval PGSTE sequence [5], its equivalent MAGR is zero and Eq. (14) can be shown to be

$$b(\mathrm{TS}+4\tau)=(\gamma g_a\delta)^2\left(\mathrm{TS}+\delta-\frac{\delta}{3}\right). \tag{18}$$

If we resort to the conventional evolution time definition, that is, by substituting $\Delta_{\mathrm{eff}}=\mathrm{TS}+2\delta$ and $\delta_{\mathrm{eff}}=2\delta$ to the bipolar PGSTE sequence, and $\Delta_{\mathrm{eff}}=\mathrm{TS}+\delta$ and $\delta_{\mathrm{eff}}=\delta$ to the Tanner PGSTE sequence, respectively, Eqs. (17) and (18) can be rewritten in their familiar form

$$b(\mathrm{TS}+4\tau)=(\gamma g_a\delta_{\mathrm{eff}})^2\left(\Delta_{\mathrm{eff}}-\frac{1}{3}\delta_{\mathrm{eff}}\right). \tag{19}$$

(iii) If we set $\delta_r=0$, the trapezoidal shaped gradient becomes a rectangular gradient and Eq. (13) can be shown to be equal to

$$\eta=-\frac{\delta^2+3\delta_1(\delta+\delta_1)}{5\delta^2+9\delta\delta_1+3\delta_1^2+12(\delta+\delta_1)\delta_2+6\delta_2^2}, \tag{20}$$

which is consistent with Eq. (21) derived by Sun et al. [8]. The authors would like to point out the graphical error in Eq. (22) of [8], and the correct expression should be

$$b(\mathrm{TS}+4\tau)=\frac{\gamma^2g_a^2\delta^2}{3}\{3(1+\eta)^2(\mathrm{TS}+2\delta_1)+2(1+3\eta)\delta+4\eta^2(2\delta+3\delta_2)\}. \tag{21}$$

This result can be shown to be equivalent to that derived by Galvosas et al. [10].

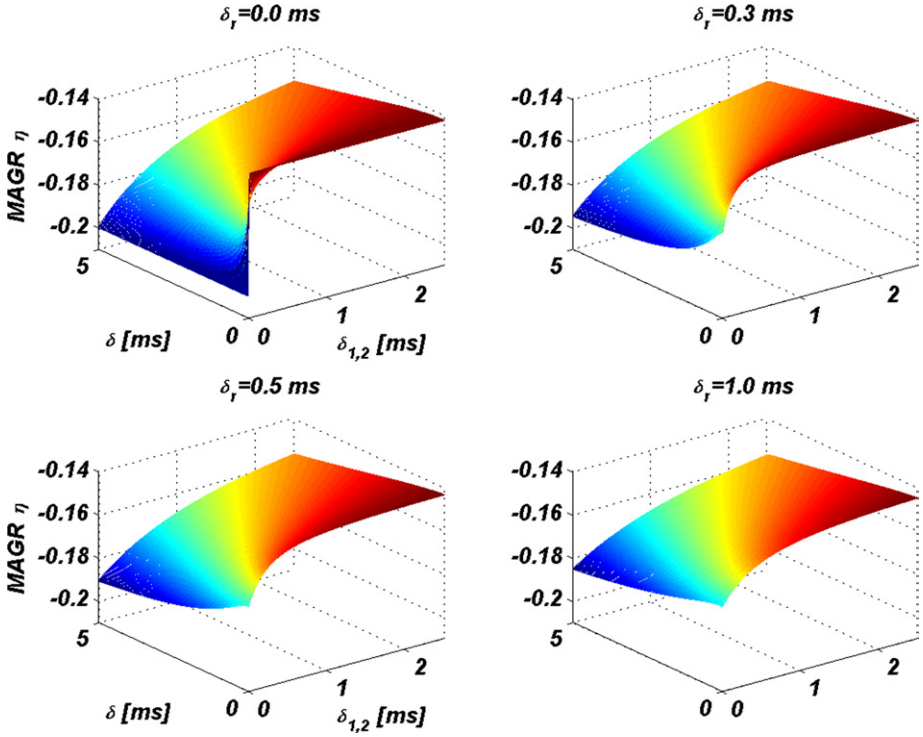

Fig. 2. The MAGR plotted as a function of the pre- and post-gradient delays δ_1, δ_2, pulsed gradient plateau duration δ, and characteristic rise time δ_r. The MAGR has a range between -0.2 and -0.14. When the trapezoidal gradient becomes rectangular ($\delta_r=0$), a large curvature can be observed. With the increment of the gradient rise time, the minimum MAGR increases and the curvature is reduced because the applied gradient is smoothed by the gradient rise time.

3. Results and discussion

According to the theory, the MAGR depends on the timing intervals during the coding period and the waveform of the applied gradients. For the case of the trapezoidal gradients, as shown in Fig. 2, its MAGR is between -0.2 and -0.14. The absolute magnitude of the MAGR for shaped gradients is smaller than that for the rectangular gradients. The range and curvature of the MAGR decrease when the shaped gradients have a longer rise time. It is important to notice that the MAGR used here and previously by Sun et al. [8,9] is the inverse of the magic pulsed field gradient (MPFG) ratio used by Galvosas et al. [10].

As shown previously, the negative MAGR value results in the two bipolar gradients having the same polarity. The effective wave-number is therefore less than the conventional bipolar gradient coding scheme. In addition, the shaped gradient has a reduced coding efficiency compared with rectangular gradients. Fortunately, for the MAGSTE sequence, the decreased coding efficiency using the shaped gradients is compensated, though not fully, by the reduced magnitude of MAGR.

4. Conclusions

The MAGSTE sequence decouples the applied gradient and the background gradients during the encoding and decoding intervals independently. It thereby enables accurate displacement measurements in complex structures where the correlation time of the background gradient is longer than the coding interval. For system with non-negligible gradient rise time, the gradient shape is smoothed and the MAGR is reduced. The reduced coding efficiency for the MAGSTE sequence using shaped gradients is compensated by the decreased MAGR magnitude.

Acknowledgment

We thank Dr. Peter van Zijl for his support and helpful comments on the manuscript.

References

[1] E.O. Stejskal, J.E. Tanner, Spin diffusion measurements: spin echoes in the presence of a time-dependent field gradient, J. Chem. Phys. 42 (1965) 288–292.
[2] C.S. Johnson, Diffusion measurement by magnetic field gradient methods, Encyclopedia of NMR, (Vol. 3) 1626-1644.
[3] J. Zhong, J.C. Gore, Studies of restricted diffusion in heterogeneous media containing variations in susceptibility, Magn. Reson. Med. 19 (1991) 276–284.
[4] R.F. Karlicek Jr., I.J. Lowe, A modified pulsed gradient technique for measuring diffusion in the presence of large background gradients, J. Magn. Reson. 37 (1980) 75–91.
[5] R.M. Cotts, T. Sun, J.T. Marker, M.J.R. Hoch, Pulsed field gradient stimulated echo methods for improved NMR diffusion measurements in heterogeneous systems, J. Magn. Reson. 83 (1989) 252–266.
[6] L.L. Latour, L. Li, C.H. Sotak, Improved PFG stimulated-echo method for the measurement of diffusion in inhomogeneous fields, J. Magn. Reson. B 101 (1993) 72–77.
[7] J.G. Seland, G.H. SØrland, K. Zick, B. Hafskjold, Diffusion measurement at long observation times in the presence of spatially variable internal magnetic field gradients, J. Magn. Reson. 146 (2000) 14–19.
[8] P.Z. Sun, J.G. Seland, D. Cory, Background gradient suppression in pulse gradient stimulated echo measurement, J. Magn. Reson. 161 (2003) 168–173.
[9] P.Z. Sun, Nuclear magnetic resonance microscopy and diffusion, Ph.D. thesis, Massachusetts Institute of Technology (2003)..
[10] P. Galvosas, F. Stallmach, J. Kärger, Background gradient suppression in stimulated echo NMR diffusion studies using magic field gradient ratios, J. Magn. Reson. 166 (2004) 164–173.
[11] A. Sodickson, D.G. Cory, A generalized k-space formalism for treating the spatial aspects of a variety of NMR experiments, Prog. NMR Spectrosc. 33 (1998) 77–108.